EnMAP Flight Campaigns

Technical Report

Isábena 2011

An EnMAP Preparatory Flight Campaign

Saskia Foerster, Arlena Brosinsky,
Charlotte Wilczok, Marcus Bauer

Recommended citation of the report:

Foerster, S.; Brosinsky, A.; Wilczok, C.; Bauer, M. (2015): Isábena 2011 - An EnMAP Preparatory Flight Campaign, *EnMAP Flight Campaigns Technical Report, GFZ Data Services.*
http://doi.org/10.2312/enmap.2015.007

Supplementary datasets:

Foerster, S.; Brosinsky, A.; Wilczok, C.; Bauer, M. (2015): Isábena 2011 - An EnMAP Preparatory Flight Campaign (Datasets), *GFZ Data Services*.
http://doi.org/10.5880/enmap.2015.007

Imprint

EnMAP Consortium

GFZ Data Services

Telegrafenberg
D-14473 Potsdam

Published in Potsdam, Germany
October 2015

http://doi.org/10.2312.enmap.2015.007

EnMAP Flight Campaigns

Technical Report

Isábena 2011

An EnMAP Preparatory Flight Campaign

Saskia Foerster, Arlena Brosinsky, Charlotte Wilczok, Marcus Bauer

GFZ German Research Centre for Geosciences

Supported by:
Federal Ministry for Economic Affairs and Energy
on the basis of a decision by the German Bundestag

Table of Contents

Abstract

The dataset is composed of a) hyperspectral imagery acquired with AISA Eagle and Hawk imaging spectrometer data in the range 400 to 2500 nm on April 2 and August 9, 2011, with a ground sampling distance of 4 m in 12 and 15 flight lines, respectively; b) airborne LiDAR data acquired in single-pulse mode in August 2011 concurrent with hyperspectral data acquisition with an avarage point density of 0.7 hits per meter squared; c) spectral reference measurements acquired with a portable ASD field spectroradiometer around the days of image acquisitions d) fractional cover of green vegetation, dry vegetation, bare soil and rock were visually estimated for 60 (April) and 53 (August) transects of 20-m length. The overall goal of the study was to investigate the potential of hyperspectral and LiDAR data for assessing sediment connectivity at the hillslope to subcatchment scale. For that the fractional cover of green vegetation, dry vegetation, bare soil and rock was derived by applying a multiple endmember spectral mixture analysis approach to the hyperspectral image data. The LiDAR point clouds were pre-processed to generate a digital elevation map as well as a vegetation height map, both with 4-m spatial resolution.

Coordinates:	**center:**	42.36 N / 0.52 E
	NW:	42.44 N / 0.47 E
	NE:	42.44 N / 0.57 E
	SE:	42.27 N / 0.57 E
	SW:	42.27 N / 0.48 E

Keywords: Hyperspectral Imagery, Airborne Laserscanning, Mediterranean drylands, Ground fractional cover

Related Work:

Information about spectral and field data processing (Wilczok 2013), LiDAR data processing (Bauer 2013), methodological approaches and final results including spatially explicit maps on ground fractional cover (green and dry vegetation, soil and rock) and index of connectivity (Foerster et al. 2014) can be found in the following documents:

Foerster, S., Wilczok, C., Brosinsky, A., Segl, K. (2014): Assessment of sediment connectivity from vegetation cover and topography using remotely sensed data in a dryland catchment in the Spanish Pyrenees. - Journal of Soils and Sediments, 14, 12, p. 1982-2000, http://doi.org/10.1007/s11368-014-0992-3.

Wilczok C. (2013): Bitemporale Analyse von Bodenbedeckungsgraden durch MESMA Entmischung von hyperspektralen fernerkundungsdaten. Diploma thesis, University of Potsdam, Germany [in German].

Bauer M. (2013): Skalenübergreifende Analyse von Fließwegen auf Basis von Geländemodellen (LiDAR und ASTER) am Beispiel des Isábena-Einzugsgebietes in Nordost Spanien. Diploma thesis, University of Potsdam, Germany [in German].

Please acknowledge the source of the airborne data, i.e. NERC-ARSF and CEDA in any publication or presentation by referring to:

NERC Airborne Research and Survey Facility (ARSF) Remote Sensing Data. CEDA-EO (2011)

1 Introduction

The Environmental Mapping and Analysis Program (EnMAP) is a German hyperspectral satellite mission that aims at monitoring and characterizing the Earth's environment on a global scale. EnMAP serves to measure and model key dynamic processes of the Earth's ecosystems by extracting geochemical, biochemical and biophysical parameters, which provide information on the status and evolution of various terrestrial and aquatic ecosystems. An overview of the EnMAP mission is provided in Guanter et al. (2015). In the frame of the EnMAP preparatory phase, pre-flight campaigns including airborne and in-situ measurements in different environments and for several application fields are being conducted. The main purpose of these campaigns is to support the development of scientific applications for EnMAP. In addition, the acquired data are input in the EnMAP end-to-end simulation tool (EeteS) and are employed to test data pre-processing and calibration-validation methods. The campaign data are made freely available to the scientific community under a Creative Commons Attribution-ShareAlike 4.0 International License. An overview of all available data is provided in the EnMAP Flight Campaigns Metadata Portal (http://www.enmap.org/?q=flightbeta).

Flight Campaign "Isábena"

The study area encompasses two subcatchments (Villacarli and Carrasquero) of the mesoscale, semi-humid Isábena catchment (445 km²) located in the southern Pyrenees in north-eastern Spain. The area is characterized by a rough terrain (650 m to 2,600 m), resulting in a pronounced climatic and land cover gradient. Strong inter-annual and seasonal variability of precipitation, temperature and local growth conditions create a highly heterogeneous landscape. The wide abundance of Miocene marls lead to the formation of badlands featuring very high erosion rates. Overall, the Isábena River is characterized by large sediment yields indicating high connectivity between the source areas and the fluvial network and resulting in severe siltation and storage capacity loss in the downstream Barasona reservoir. Connectivity processes (i.e. the ease with which sediment can move through a catchment) play an important role in the redistribution of water and sediments. Apart from topography, vegetation cover is one of the main factors driving sediment connectivity, particularly the patchy vegetation cover typical of many dryland environments.

To assess the sediment connectivity for two adjacent subcatchments (~70 km²) of the Isábena River in contrasting seasons, hyperspectral imagery (AISA Eagle and Hawk) was acquired in April and August 2011, respectively, with simultaneous comprehensive field surveys. In addition, airborne LiDAR data (Leica ALS50) was acquired during the August 2011 campaign. Fractional cover of green and dry vegetation, bare soil and rock were visually estimated for 60 (April) and 53 (August) transects of 20-m length. Nadir photographs were taken, land use type was recorded and vegetation height and major species composition were estimated for each transect. Spectral reflectance signatures were collected for 25 (April) and 23 (August) transects (ASD High-Res3, ASD Inc., Boulder, CO) when weather conditions allowed.

2 Data Acquisition

Hyperspectral imagery was acquired during two flight campaigns operated by NERC ARSF. Airborne Imaging Spectrometer for Application (AISA) Eagle and Hawk imaging spectrometer data (Specim Ltd., Oulu, Finland) were acquired at the altitude of 4,200 m on April 2 and August 9, 2011, with a ground sampling distance (GSD) of 4 m in 12 and 15 flight lines, respectively (see Figure 3.1). Details on the flight lines can be found in table 2.1 and 2.2.

Airborne LiDAR data was acquired with a Leica ALS50 instrument in single-pulse mode (maximum of four returns per given pulse recorded) in August 2011 concurrent with hyperspectral data acquisition. The average flight altitude of 4,200 m resulted in an average point density of 0.7 hits per m². The mean error magnitude was 3.3 cm with a standard deviation of 4.1 cm for 2,500 m altitude, with an additional maximum error of 10–15 cm at the edges of the swath due to a systematic roll boresight bias (NERC 2011a).

2.1 Campaign April 2011

Time: April 2, 2011 start: 08:44 end: 12:40 (Universal Time)
Samples: 953 (Eagle), 320 (Hawk)
Bands: 255 (Eagle), 256 (Hawk)
Wavelengths: 129.20 (399.97) - (998.46) 1328.01 nm (Eagle), 907.68 - 2516.28 nm (Hawk)
Binning: Spatial 1 Spectral 2 (Eagle), Spatial 1 Spectral 1 (Hawk)
FOV: 37.7 (Eagle), 24.0 (Hawk)

Table 2.1: Details of the flight lines recorded in April 2011

Strip Number	Flight Altitude	Scan Frequency	Flight Heading	Solar Azimuth	Solar Zenith	Pixel Size (E/H)*	Lines (E/H)*
e/h09212	4187 m	30.0 Hz	185°	150.8°	40.9°	2 m / 4 m	8261/ 8261
e/h09211	4173 m	30.0 Hz	346°	148.3°	41.5°	2 m / 4 m	8135/ 8136
e/h09210	4154 m	30.0 Hz	183°	146.0°	42.2°	2 m / 4 m	8472/ 8474
e/h09209	4156 m	30.0 Hz	350°	143.3°	43.1°	2 m / 4 m	8826/ 8827
e/h09208	4164 m	30.0 Hz	182°	140.7°	44.0°	2 m / 4 m	8687/ 8688
e/h09207	4207 m	30.0 Hz	353°	138.6°	44.8°	2 m / 4 m	8336/ 8337
e/h09206	4195 m	30.0 Hz	186°	136.5°	45.7°	2 m / 4 m	8674/ 8647
e/h09205	4171 m	30.0 Hz	350°	134.1°	46.7°	2 m / 4 m	9000/ 9001
e/h09204	4162 m	30.0 Hz	184°	132.1°	47.7°	2 m / 4 m	9020/ 9021
e/h09203	4192 m	30.0 Hz	351°	129.9°	48.8°	2 m / 4 m	8633/ 8634
e/h09202	4177 m	30.0 Hz	186°	127.8°	49.9°	2 m / 4 m	8689/ 8691
e/h09201	4178 m	30.0 Hz	350°	125.7°	51.1°	2 m / 4 m	9722/ 9752

**(E/H) refers to Eagle (E) and Hawk (H) data*

2.2 Campaign August 2011

Time: August 09, 2011 start: 9:37 end: 12:37 (Universal Time)
Samples: 953 (Eagle), 320 (Hawk)
Bands: 255 (Eagle), 233 (Hawk)
Wavelengths: 129.20 (399.97) – (998.46) 1328.01 nm (Eagle), 1002.30 - 2465.81 nm (Hawk)
Binning: Spatial 1 Spectral 2 (Eagle), Spatial 1 Spectral 1 (Hawk)
FOV: 37.7 (Eagle), 24.0 (Hawk)

Table 2.2: Details of the flight lines recorded in August 2011

Strip Number	Flight Altitude	Scan Frequency	Flight Heading	Solar Azimuth	Solar Zenith	Pixel Size (E/H)*	Lines (E/H)*
e/h22116	4253 m	30.0 Hz	350°	176.3°	26.6°	2 m / 4 m	9303/ 9304
e/h22115	4215 m	30.0 Hz	189°	172.6°	26.7°	2 m / 4 m	8821/ 8822
e/h22114	4251 m	30.0 Hz	352°	168.4°	27.0°	2 m / 4 m	8853/ 8854
e/h22113	4245 m	30.0 Hz	185°	164.3°	27.3°	2 m / 4 m	8754/ 8756
e/h22112	4253 m	30.0 Hz	351°	160.7°	27.7°	2 m / 4 m	8991/ 8992
e/h22111	4250 m	30.0 Hz	188°	156.8°	28.2°	2 m / 4 m	8877/ 8878
e/h22110	4255 m	30.0 Hz	353°	153.0°	28.9°	2 m / 4 m	8407/ 8409
e/h22109	4250 m	30.0 Hz	185°	149.8°	29.5°	2 m / 4 m	9167/ 9169
e/h22108	4249 m	30.0 Hz	351°	146.7°	30.2°	2 m / 4 m	4788/ 4789
e/h22107	4243 m	30.0 Hz	187°	142.9°	31.1°	2 m / 4 m	8554/ 8555
e/h22106	4245 m	30.0 Hz	351°	140.1°	31.9°	2 m / 4 m	8043/ 8044
e/h22105	4248 m	30.0 Hz	187°	137.0°	32.9°	2 m / 4 m	12407/12408
e/h22104	4246 m	30.0 Hz	351°	134.5°	33.8°	2 m / 4 m	8212/ 8226
e/h22103	4248 m	30.0 Hz	189°	131.6°	34.9°	2 m / 4 m	8374/ 8376
e/h22117	4239 m	30.0 Hz	186°	180.9°	26.6°	2 m / 4 m	8438/ 8439

**(E/H) refers to Eagle (E) and Hawk (H) data*

3 Data Processing and Products

3.1 Hyperspectral data

Level 1[1]: The data are delivered as Level 1b ENVI BIL format files by NERC ARSF, meaning that radiometric calibration algorithms have been applied and navigation information has been synced to the image data.

Level 2[1]: Bad pixels were removed from AISA Hawk data (automatic detection using in-house software followed by manual control). Ortho-rectified radiance data were derived using in-house software in combination with a digital terrain model (DEM derived from LiDAR data, 2m and 4m spatial resolution, respectively) for Eagle and Hawk data separately. Subsequently, Eagle and Hawk images were fused with the Eagle image resampled to Hawk resolution and the overlap range (970-1000 nm) corrected using in-house software. Level 2 geo products were corrected for atmospheric influences using Atcor4 (rugged terrain option). Then, individual flight lines were mosaicked using ENVI 4.8 and the outer orientation was adjusted to a reference Orthophoto using 120 Ground Control Points (ArcGIS 10.0).

[1] Data levels used here are out-dated and not in line with the future EnMAP data levels.

Water vapour bands were removed (1336 – 1425 nm and 1790-1935 nm) so that both mosaics contained 450 bands. Subsequently, an empirical line post-calibration [ELI] was applied using field spectra collected during overflight for the April mosaic. Due to insufficient ground reflectance data, the August mosaic was adapted to the April mosaic using ELI. More detailed information can be found in Wilczok (2013).

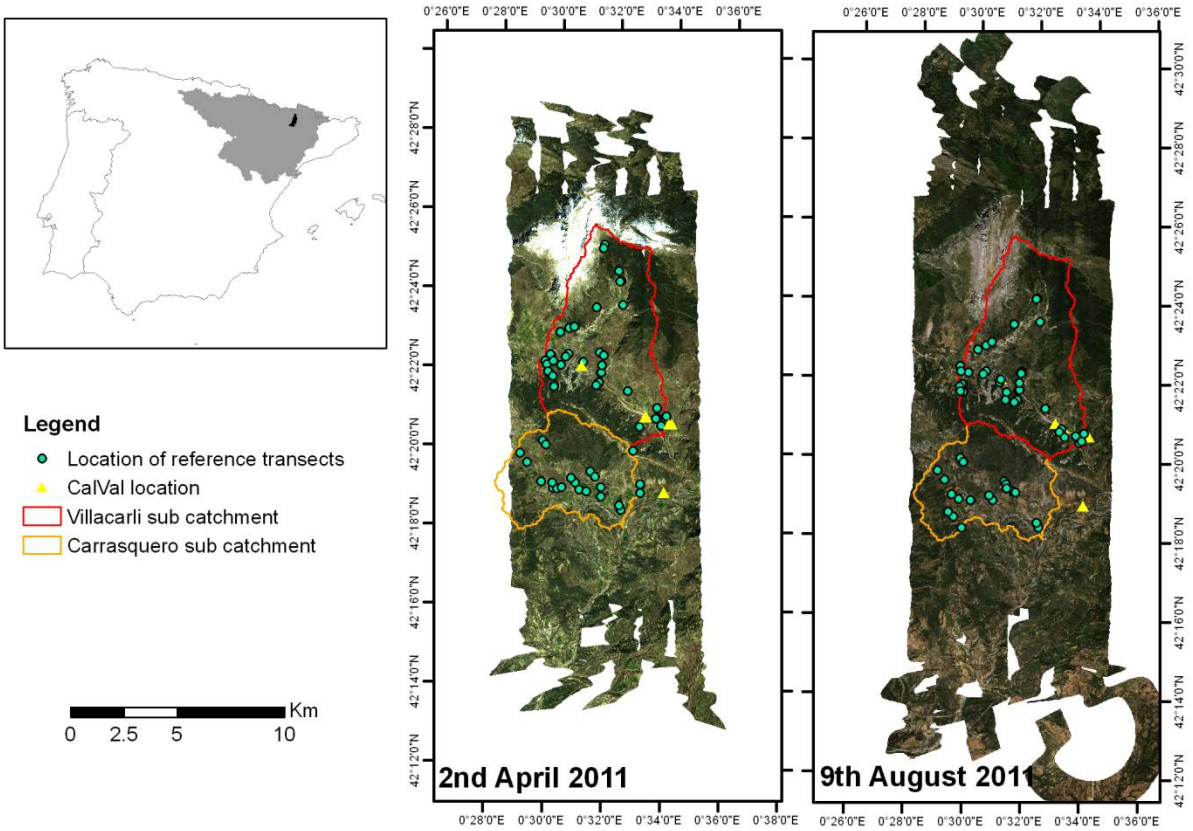

Figure 3.1: AISA flight lines locations and covered field plots for terrestrial surveys of vegetation coverage and spectral reflectance.

3.2 Simulated EnMAP data

Simulated EnMAP data were generated using the EnMAP end-to-end simulation software (Segl et al., 2012), Figure 3.2.

3.3 LiDAR data

"Preprocessing of the LiDAR point clouds was carried out by the Institute for Earth and Environmental Sciences at the University of Potsdam (Bauer 2013) applying LAStools (Martin Isenburg, rapidlasso GmbH, rapidlasso.com). It comprised the classification of the point cloud into ground and non-ground points and the generation of a digital elevation map (DEM; including only ground points) as well as a vegetation height map, both with 4-m spatial resolution. In a further step, the DEM was hydrologically corrected for local pits using Terrain Analysis Using Digital Elevation Models (TauDEM 5.0, hydrology.uwrl.usu.edu/taudem/taudem5.0/index.html)." (Foerster et al. 2014).

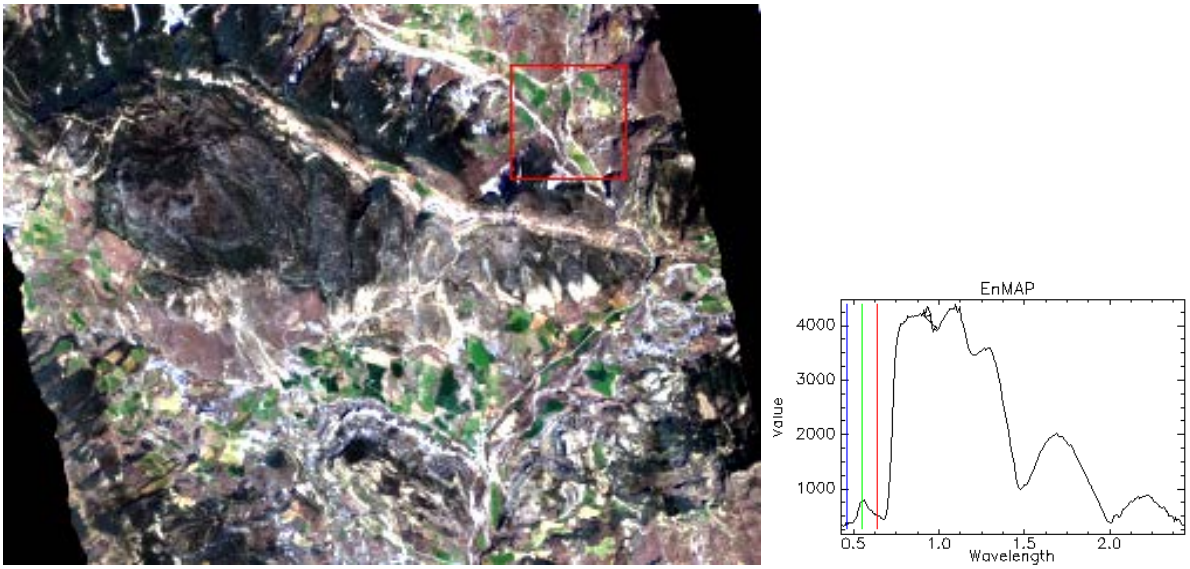

Figure 3.2: Simulated EnMAP image derived from the AISA image of the Isábena area from 2nd April 2011.

4 File Description

4.1 File Format

Band Sequential Image File [*.bsq] and file header [*.hdr]

4.2 Data content and structure

Image files are described in the header file by the following attributes:
ENVI description, samples, lines, bands , header offset, file type, data type, interleave, sensor type, byte order, map info, wavelength units, band names, wavelength, fwhm.

5 Data Quality/Accuracy

5.1 Hyperspectral data

A detailed assessment of raw data quality can be found in NERC (2011b). Timing errors (order of 0.05s) that may occur from an error in the synchronisation between the navigation system and the Eagle and Hawk sensors due to a fault in the Specim system were corrected manually prior to delivery. NERC ARSF advises caution when examining spectral responses at the edges of the usable range as the signal to noise ratio appears to degrade at the low and high wavelength limits of both sensors (Eagle data < 450 nm or > 900 nm and Hawk data < 1100 nm and > 2400 nm) (NERC 2011b).

Since the LiDAR data covers a smaller area than the hyperspectral data, LiDAR DEMs were patched on a resampled ASTER DEM for use during the geocorrection of the hyperspectral image data. This results in visible striping of the outer margins of the corrected mosaic.

After the adjustment to an Orthophoto described in chapter 3.1, the RMSE was < 4 m. However, due to the rough terrain, geometric accuracy varies within the image mosaics (0-8 m), whereas distortions are mainly visible along the overlap of flight lines. No systematic displacements were observed.

Unfortunately, the application of ELI did not allow for a comparison of airborne and simultaneously collected ground reflectance data for an assessment of spectral accuracy.

5.2 Simulated EnMAP data

The quality of simulated EnMAP data is related to the quality of the AISA data that the simulation was based on. The EnMAP VNIR detector records data up to 1000 nm while the SWIR-detector records data from 900 nm, resulting in some bands in the 900 – 1000 nm range being recorded twice by two different detectors, whereas their spectral information may slightly differ (see Fig.3.2).

5.3 LiDAR data

A detailed assessment of raw data quality can be found in NERC (2011a). From a comparison between LiDAR data and GCPs, NERC (2011a) reports a mean error magnitude of 2.4-2.9 cm and evidence of a systematic roll boresight error (10-15cm in magnitude). Since there were some problems with the LiDAR point clouds of flight lines 1 and 2, only flight lines 3-15 were processed at the University of Potsdam (Bauer 2013). However, 2 m and 4 m LiDAR DEMs patched to ASTER scenes are available from NERC for geometric correction of AISA flight lines.

6 Additional Data

6.1 Additional GIS Data

A GIS data base was set up including maps, field data and additional environmental background information that were collected from past studies in the years from 2005 to 2015 grouped according the following categories[2].

Table 6.1: Additional GIS data

GIS Data Category	Dataset Examples	Acquisition Time
Soil	soil map 1:1,000,000	1986
Lithology	Lithological map 1:200,000	1997
Permanent Observations	rainfall, temperature, River discharge, suspended sediment concentration	from 1941; 2005-2015
Digital Terrain Model	15 and 30 m ASTER DEM contour lines	2006 2012
landuse	Landuse map 1:50,000	1980 and 2008
Remote Sensing	Orthophotos, Aerial Photographs Rapid Eye Landsat	before 2012 1956 - 1985, 1995 2009-2011 2000-2003
Buildings	Buildings, streets, rivers	before 2012
Boundaries	Catchment boundaries	2005

[2] These data will not be part of the data package, but may be provided upon request on a case-by-case decision depending on individual licence agreements.

6.2 Additional Spectral Field/ Lab Measurements

Spectral measurements were conducted with an ASD FieldSpec3 High-Res portable spectro-radiometer (ASD, Inc., Boulder, CO) delivering relative reflectance values in relation to a white reference standard (95 % Zenith Alucore Reflectance Target, SphereOptics GmbH, Uhldingen, Germany). Spectral reflectance values were recorded between 350 and 2500 nm within spectral intervals resampled to 1 nm wavelength units.
Field plots were sampled a) along transects (see chapter 6.3) with five readings per 1 m² plot at a constant height of 1.4 m over ground, resulting in a sensor footprint diameter of 0.2 m. For every reading a reflectance curve was generated by averaging 50 single measurements under constant viewing geometry. In addition, field plots were sampled b) for calibration and validation purposes simultaneously with airborne data acquisition. Therefore, 30 single readings were collected from 15 m x 15 m homogeneous areas, again averaging 50 measurements per reading. More detailed information can be found in Wilczok (2013).

6.3 Additional Field Data

Additional field data were sampled in 13 days (April and August, respectively) around airborne acquisitions in the Villacarli and Carrasquero subcatchments (approx. 70 km²). Supplementary data include information on location (GPS) and time of data acquisition, (recent) weather conditions, and general site conditions (slope, exposition, soil colour, moisture). Sixty (April) and 53 transects (August) were sampled, covering the landuse classes forest, agricultural land, grassland, shrubland, badland and riverbed. Each transect was 20 m in length, and samples were taken for 1 m x 1 m plots every 2 m (1 m, 3 m, 5 m, 7 m, 9 m, 11 m, 13 m, 15 m, 17 m, 19 m). Extended samples were taken every 4 m (3 m, 7 m, 11 m, 15 m, 19 m). Transects were arranged parallel to hillslopes at representative sites (homogeneous and of a size of at least 50 m x 50 m). Arable fields were only sampled along the edges of fields to reduce disturbance of crops. Samples at 2 m included fractional cover estimates of green vegetation (GV), dry vegetation assumed to be photosynthetically non-active (NPV), bare soil and rock. Visual estimation was carried out in 10 % steps for 1 m² plots using the quadrate sampling method (Kreeb 1983, Coulloudon et al. 1999, Kercher et al. 2003). Estimates were averaged for each transect. Nadir photographs of each estimation site were taken. Extended sampled at 4 m included measurements of vegetation height (min, mean, max), grab samples of surface soil (top 2 cm, approx. 500 g per transect), a description of vegetation composition (trees, shrubs, grass/herbs, mosses), and species composition (dominant species). If weather conditions allowed (cloudless, max. 3 hours before/ after solar noon) field reflectance spectra were taken using an ASD FieldSpec3 High-Res portable spectroradiometer (ASD, Inc., Boulder, CO). On forested stands, a 10 m diameter (5 m radius) circle was selected from the centre (10 m mark) of each transect. All trees within this circle were measured (height and diameter at breast height) and identified (species). For further information please refer to Foerster et al. (2014) and Wilczok (2013).

6.4 Additional Laboratory Data

Grain size distribution was analysed by dry sieving (> 2mm), wet sieving (> 63 µm) and laser diffraction (< 63 µm) for material from 19 transects.

7 Dataset Contact

Karl Segl
Email: karl.segl@gfz-potsdam.de
Phone: +49 (0) 331 288 1193

Saskia Foerster
Email: saskia.foerster@gfz-potsdam.de
Phone: +49 (0) 331 288 28615

8 Acknowledgements

This research was carried out within the project “Generation, transport and retention of water and suspended sediments in large dryland catchments: monitoring and integrated modelling of fluxes and connectivity phenomena” funded by the Deutsche Forschungsgemeinschaft (DFG) and the Federal Ministry of Economics and Technology (BMWi, 50EE0946). AISA data acquisition was conducted by the National Environment Research Council Airborne Research and Survey Facility (NERC-ARSF, UK) and funded by EUFAR Transnational Access (April) and by BMWi (August). The authors would like to thank Randolf Klinke, Arne Brauer, Simon Hörhold, Elfrun Lindenthal, Charlotte Wilczok and Marcus Bauer for their support in the field, and Marcus Bauer and Theo Becker for support in preprocessing the LiDAR data.

9 References

Bauer M (2013) Skalenübergreifende Analyse von Fließwegen auf Basis von Geländemodellen (LiDAR und ASTER) am Beispiel des Isábenaeinzugsgebietes in Nordost Spanien. Diploma thesis, University of Potsdam, Germany [in German].

Coulloudon B, Eshelman K, Gianola J, Habich N, Hughes L, Johnson C, Pellant M, Podborny P, Rasmussen A, Robles B, Shaver P, Spehar J, Willoughby J (1999) Sampling vegetation attributes. Interagency Technical Reference/ U.S. Department of the Interior, Bureau of Land Management, Denver, Colorado, USA.

Foerster, S., Wilczok, C., Brosinsky, A., Segl, K. (2014): Assessment of sediment connectivity from vegetation cover and topography using remotely sensed data in a dryland catchment in the Spanish Pyrenees. - Journal of Soils and Sediments, 14, 12, p. 1982-2000. http://doi.org/10.1007/s11368-014-0992-3.

Guanter, L., Kaufmann, H., Segl, K., Foerster, S., Rogaß, C., Chabrillat, S., Küster, T., Hollstein, A., Rossner, G., Chlebek, C., Straif, C., Fischer, S., Schrader, S., Storch, T., Heiden, U., Mueller, A., Bachmann, M., Mühle, H., Müller, R., Habermeyer, M., Ohndorf, A., Hill, J., Buddenbaum, H., Hostert, P., van der Linden, S., Leitão, P., Rabe, A., Doerffer, R., Krasemann, H., Xi, H., Mauser, W., Hank, T., Locherer, M., Rast, M., Staenz, K., Sang, B. (2015): The EnMAP Spaceborne Imaging Spectroscopy Mission for Earth Observation. - Remote Sensing, 7, 7, p. 8830-8857. http://doi.org/10.3390/rs70708830.

Kercher SM, Frieswyk CB, Zedler JB (2003) Effects of sampling teams and estimation methods on the assessment of plant cover. Journal of Vegetation Science 14:899–906. http://doi.org/10.1658/1100-9233(2003)014[0899:EOSTAE]2.0.CO;2.

Kreeb KH (1983) Vegetationskunde. Methoden und Vegetationsformen unter Berücksichtigung Ökosystemischer Aspekte. Ulmer, Stuttgart.

Natural Environment Research Council (NERC) (2011a) Lidar data quality overview, http://arsf-dan.nerc.ac.uk/trac/wiki/Reports (Accessed August 2013).

Natural Environment Research Council (NERC) (2011b) Hyperspectral data quality report (overview of any issues with data), http://arsf-dan.nerc.ac.uk/trac/wiki/Reports (Accessed October 2015).

Segl K, Guanter L, Rogass C, Kuester T, Roessner S, Kaufmann H, Sang B, Mogulsky V, Hofer S (2012) EeteS - The EnMAP End-to-End Simulation Tool. IEEE Journal of Selected Topics in Applied Earth Observations and Remote Sensing 5: 522–530. http://doi.org/10.1109/JSTARS.2012.2188994.

Wilczok C. (2013): Bitemporale Analyse von Bodenbedeckungsgraden durch MESMA Entmischung von hyperspektralen Fernerkundungsdaten. Diploma thesis, University of Potsdam, Germany [in German].

10 Appendix

List of available datasets

The data made available with this report is listed in table 10.1. Unless otherwise stated, all data are delivered in UTM WGS84 Zone 31N.

Table 10.1: Description of the available data; if there are separate files for April and August this will be indicated by the file name (..._april and ..._august, respectively)

Data	Description	File name	Type	Folder	April	August
AISA	airborne level1b	flightline*	bil, hdr	AISA_L1	x	x
	navigation information	flightline*	bil, hdr	AISA_L1	x	x
	airborne level2	AISA_	bsq, hdr	AISA_L2	x	x
EnMAP	simulated from AISA	simEnMAP_	bsq, hdr	simEnMAP	x	x
LiDAR	Raw data	flightline*	las	LiDAR	NA	x
	DEM (4 m spatial resolution)	DEM_4m	tif	LiDAR	NA	x
	DEM (4 m spatial resolution, pit filled)	DEM_4mfel	tif	LiDAR	NA	x
field spectra	CalVal during overflight	ASD_cv_mean_nj_	esl, hdr	ASD	x	x
	transects	ASD_mean_nj_	esl, hdr	ASD	x	x
photos	photographs	photo numbers**	jpg	photos	x	x
field survey	field protocol (overview transects, cover estimates, photo numbers, spectral reflectance measurements, tree meas.)	field data	xls	xls	x	x
lab analyses	lab protocol (grain size distribution)	lab_gsd	xls	xls	x	x

*as given in table 2.1 and 2.2 of this report

**as given in file “field_data”